Electronic Supplementary Material (ESI) for Dalton Transactions.

Towards the Rational Design of the Py5–Ligand Framework for Ruthenium–Based Water Oxidation Catalysts

Mauro Schilling[a], Michael Böhler[a], and Sandra Luber[a*]

[a] *University of Zurich, Department of Chemistry C, Winterthurerstrasse 190, CH-8057 Zurich, Switzerland. E-mail: sandra.luber@chem.uzh.ch*

1 Methods

Calculations were carried out using the Turbomole software package[1] (version 7.0). Geometry optimizations and frequency analyses were performed employing (unrestricted) Kohn-Sham density functional theory with the BP86 exchange-correlation functional[2,3], the def2-TZVP basis set[4] (with the corresponding 28 electron effective core potential for Ru) and Grimme's D3 dispersion correction[5] (no Becke-Johnson damping). Single-point electronic energies were obtained with B3LYP-D3[6,7]/def2-TZVP and the COSMO solvation model[8] (dielectric constant $\varepsilon = 80$ for water, default radii). *Kang et al.* exhaustively benchmarked the performance of different exchange-correlation functionals against coupled cluster singlet doublet (triplet) CCSD(T) calculations. While for each reaction a different functional performed best, B3LYP was found to produce reasonable results for the O$-$O bond formation.[9] Calculations were sped-up by means of the Resolution-of-the-Identity approach (RI-J, with its corresponding basis set[10–12]) and Multipole-Assisted-RI-J[13] (MARIJ). Gibbs free-energy corrections were obtained from the normal mode analysis, based on the rigid-rotor, harmonic oscillator approximations, using the Turbomole module freeh at a pressure of 1 bar and a temperature of 298.15 K; no scaling factor was applied to the vibrational frequencies. The Gibbs free energies were furthermore corrected for the change in standard state from 1 bar to 1 M by adding $1.90\,\mathrm{kcal\,mol^{-1}}$ (resp. 1 bar to 55.6 M for water, $4.28\,\mathrm{kcal\,mol^{-1}}$). Deprotonations include the solvation free energy of a proton (but not its translational free energy) of $265.9\,\mathrm{kcal\,mol^{-1}}$; reduction potentials are given relative to the standard hydrogen electrode (SHE) which was taken to be 4.28 V[14–16]. The standard reduction potential was calculated as given below, where n is the number of electrons transferred, F is the Faraday constant, $\Delta G^{\circ}_{\mathrm{reduction}}$ the Gibbs free energy change of the reduction and $E^{\mathrm{absolute}}_{\mathrm{SHE}}$ the absolute reduction potential of the SHE:

$$\Delta E^{\circ}_{\mathrm{reduction}} = \frac{\Delta G^{\circ}_{\mathrm{reduction}}}{n\mathrm{F}} - E^{\mathrm{absolute}}_{\mathrm{SHE}}. \tag{1}$$

Proton-coupled electron transfer reactions include the energy of half a hydrogen molecule[17] whose Gibbs free energy correction consists of the zero-point vibrational energy plus a thermal correction of 0.52 eV[18]. For comparison with the ideal catalyst (and only there), PCET free energies were scaled by 0.807 which is the ratio of the computational and the experimental free energy for water oxidation with our settings. Larger basis sets were used to calculate single-point electronic energies (def2-TZVPP, def2-QZVP) but did not influence the relative energies significantly. Electronic contributions of the multiplicity on the ground state was neglected when computing the Gibbs free energy as it would amount to only $0.41\,\mathrm{kcal\,mol^{-1}}$ for doublet states and $0.65\,\mathrm{kcal\,mol^{-1}}$ for triplet states.

1.1 Bond Scans

The scans were done with geometries optimized at the BP86-D3/def2-SVP level and B3LYP-D3/def2-TZVP single-points. A good nuclear structure can usually be obtained already on the def2-SVP level and for our scans the reduced computational time was crucial. All scans were calculated as restricted singlets on the Ru(II) oxidation state and a step-width of 0.1 Bohr was used around the equilibrium geometry (3.3 to 5.0 Bohr) and 0.2 Bohr for the rest. For the electronic energy calculations (in the def2-TZVP basis) the proper propagation of the orbital guess for the self-consistent field procedure and damping proved to be critical in order to obtain smooth curves.

1.2 Oxygen in *cis* Position to Chloride

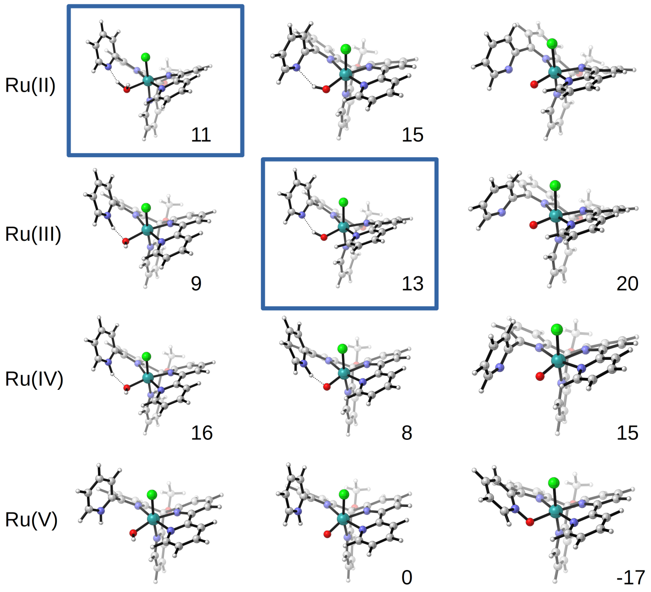

Fig. S 1 Isomers of complexes with the Py5OMe ligand where the entering water molecule is in *cis* position to the chloride. Energies are given in $\mathrm{kcal\,mol^{-1}}$, relative to the structures with the oxygen *trans* to chloride (B3LYP-D3/def2-TZVP/COSMO//BP86-D3/def2-TZVP). Structures are sequentially deprotonated from left to right. It is noticeable that in these arrangements the proton is more likely to shift from the oxygen to the pyridyl fragment. Highlighted with blue rectangles are two of the structures of the thermodynamic cycle which are comparable for *cis* and *trans* in terms of oxidation state and protonation pattern. The energies of the *cis* isomers are higher than those for the *trans* isomers, therefore it is unlikely that the catalytic cycle involves any of the above species. Notice how in the Ru(V)−O structure the ligand strain has led to a nucleophilic attack on the oxygen. This might be an artifact of the absence of explicit solvent molecules.

2 Oxygen Evolution

Because of the large dependence on explicit solvation, structures with one more additional solvent molecule for the TS of Py5OMe were prepared and optimized (3 water molecules = 1 for WNA + 2 for solvation). We limited ourselves to structures where the second explicit water molecule belongs to the first solvation shell as seen in Figure S2. The activation energies for these structures are quite similar to those obtained with only one explicit solvent molecule ($15.6\,\mathrm{kcal\,mol^{-1}}$) and are in the range of 14.3 to $17.1\,\mathrm{kcal\,mol^{-1}}$ with respect to the separated reactants, or between 5 to $10\,\mathrm{kcal\,mol^{-1}}$ with respect to the associated complex (Table 2). Regarding the value with respect to the separated reactants, it appears that there is no need for a second explicit water molecule as the activation energies are quite similar. However, with static calculations, it is in general difficult to meaningfully sample all possible starting guesses. The structures with two explicit solvent molecules resemble those with only one very much, because we used them as starting guesses. Therefore, with different starting guesses one might obtain other structures with a significantly different pattern which may lead to other values for the activation energies. For such a task molecular dynamics or other techniques may be more suitable.

Ligand	Ru(II)-Py	Ru(III)-Py	Ru(II)-Cl	Ru(III)-Cl
Py5Me	14.2	11.5	7.6	19.5
Py5OMe	4.4	1.4	8.4	21.6
Py5Et	7.3	3.6	7.8	20.3

Table S 1 Energies ($\mathrm{kcal\,mol^{-1}}$) of chlorido-water exchange (Ru-Cl) and the pyridine-water exchange (Ru-py) with the different ligands and the complexes with ruthenium in oxidation state II or III (values for Py5OMe and Py5Me were previously reported in[19]).

Variant	AR	TS	AP
A	7.1	14.3	7.1
B	10.5	15.1	7.8
C	10.9	17.1	8.2

Table S 2 Energies ($\mathrm{kcal\,mol^{-1}}$) of WNA structures with Py5OMe containing two explicit water molecules. Energies are given relative to the free OMe$-$N$^4-$Ru(V)$-$O$-$Cl complex and three free water molecules. AR = associated reactants, TS = transition state, AP = associated products.

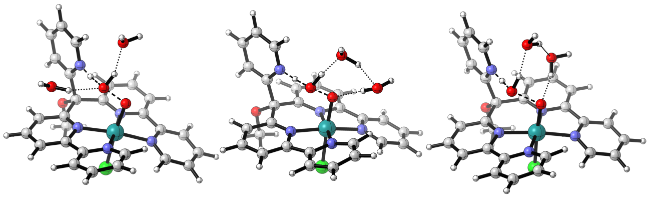

Fig. S 2 Transition-states for OMe$-$N$^4-$Ru(V)$-$O$-$Cl with two explicit water molecules in the first solvation shell. From left to right: variant A, B and C.

3 Dissociation Scans

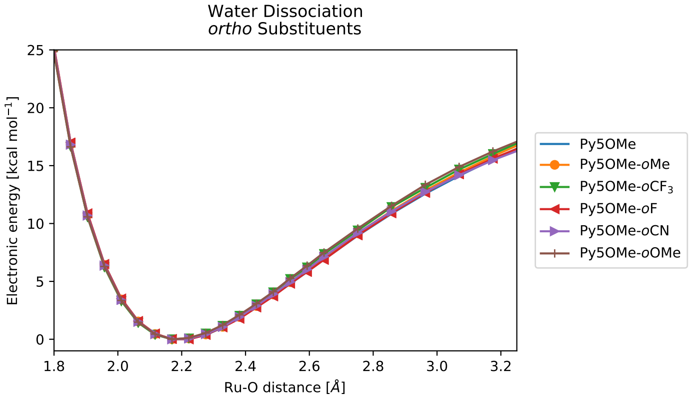

Fig. S 3 Water dissociation scans with the indicated substituents in the *ortho* position of the axial pyridine.

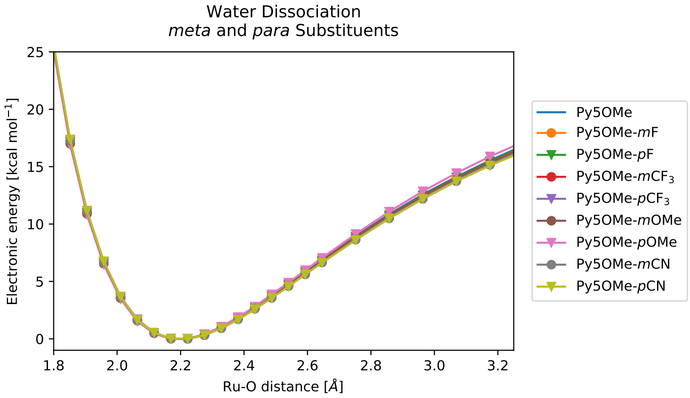

Fig. S 4 Water dissociation scans with the indicated substituents in *meta* and *para* positions of the axial pyridine.

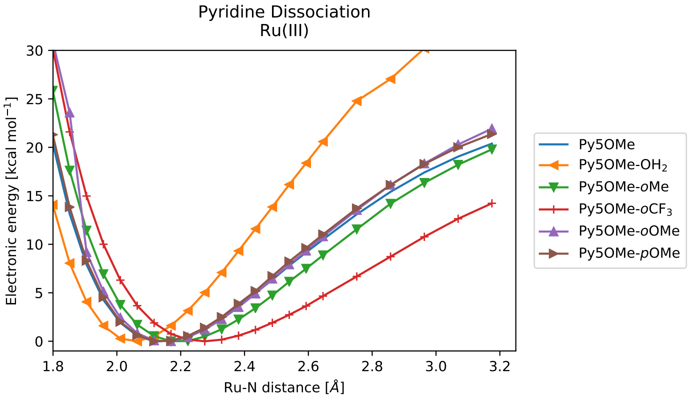

Fig. S 5 Pyridine dissociation scans on Ru(III). Note the preserved energy ordering (as in Ru(II)) *ortho*-CF$_3$ < *ortho*-Me < Py5OMe ≈ *ortho*-OMe ≈ *para*-OMe < Py5Me. The *trans*-aqua species are also included.

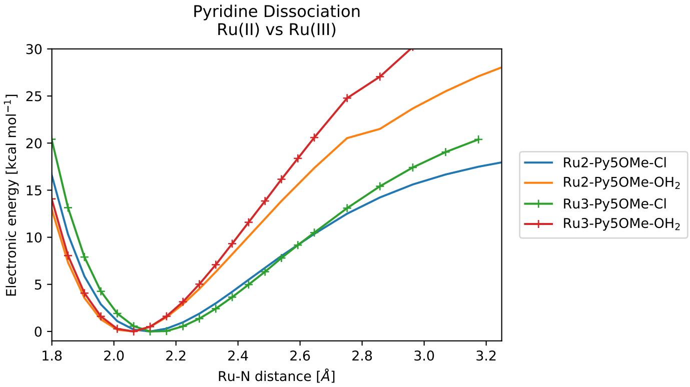

Fig. S 6 Pyridine dissociations scans comparing Ruthenium in oxidations states II and III. OH$_2$ and Cl stand for the ligand in *trans* position.

4 WNA Correlation

WNA correlation

Mod.	AR	TS	AP	Ru-spin (x10)	O-spin (x10)	LUMO (x20)	d(N-O)
o-OMe	7.30	14.84	7.69	5.25	4.46	-3.95	2.63
m-OMe	6.46	14.48	6.14	6.26	3.79	-3.81	2.41
p-OMe	6.17	11.71	3.22	7.58	2.84	-3.72	2.36
o-F	7.18	17.10	15.50	4.98	4.68	-4.04	2.71
m-F	6.78	14.67	10.35	5.72	4.06	-3.91	2.48
p-F	6.50	13.45	7.68	6.09	3.76	-3.87	2.44
o-CF$_3$	9.23	20.86	17.11	5.02	4.66	-4.03	2.69
m-CF$_3$	7.33	16.35	11.61	5.63	4.12	-3.92	2.47
p-CF$_3$	6.54	14.79	10.32	5.83	3.95	-3.91	2.46

Table S 3 Energies for AR, TS and AP in $\mathrm{kcal\,mol^{-1}}$; Mulliken spin-densities for Ru(V)=O complex (scaled by 10), LUMO energy (eV, scaled by 20); distance of pyridine-N to oxo in Å.

Notes and references

1 R. Ahlrichs, M. Bär, M. Häser, H. Horn and C. Kölmel, *Chem. Phys. Lett.*, 1989, **162**, 165–169.

2 A. D. Becke, *Phys. Rev. A*, 1988, **38**, 3098–3100.

3 J. P. Perdew, *Phys. Rev. B*, 1986, **33**, 8822–8824.

4 F. Weigend and R. Ahlrichs, *Phys. Chem. Chem. Phys.*, 2005, **7**, 3297–3305.

5 S. Grimme, J. Antony, S. Ehrlich and H. Krieg, *J. Chem. Phys.*, 2010, **132**, 154104.

6 A. D. Becke, *J. Chem. Phys.*, 1993, **98**, 5648.

7 C. Lee, W. Yang and R. G. Parr, *Phys. Rev. B*, 1988, **37**, 785–789.

8 A. Klamt and G. Schüürmann, *J. Chem. Soc., Perkin Trans. 2*, 1993, 799–805.

9 R. Kang, J. Yao and H. Chen, *J. Chem. Theory Comput.*, 2013, **9**, 1872–1879.

10 K. Eichkorn, O. Treutler, H. Öhm, M. Häser and R. Ahlrichs, *Chem. Phys. Lett.*, 1995, **240**, 283–290.

11 K. Eichkorn, F. Weigend, O. Treutler and R. Ahlrichs, *Theor. Chem. Accounts Theory, Comput. Model. (Theoretica Chim. Acta)*, 1997, **97**, 119–124.

12 F. Weigend, *Phys. Chem. Chem. Phys.*, 2006, **8**, 1057–1065.

13 M. Sierka, A. Hogekamp and R. Ahlrichs, *J. Chem. Phys.*, 2003, **118**, 9136–9148.

14 M. D. Tissandier, K. A. Cowen, W. Y. Feng, E. Gundlach, M. H. Cohen, A. D. Earhart, J. V. Coe and T. R. Tuttle, *J. Phys. Chem. A*, 1998, **102**, 7787–7794.

15 C. P. Kelly, C. J. Cramer and D. G. Truhlar, *J. Phys. Chem. B*, 2006, **110**, 16066–16081.

16 A. V. Marenich, J. Ho, M. L. Coote, C. J. Cramer, D. G. Truhlar, A. V. Marenich, J. Ho, M. L. Coote, C. J. Cramer and D. G. Truhlar, *Phys. Chem. Chem. Phys.*, 2014, **16**, 15068.

17 J. K. Nørskov, J. Rossmeisl, A. Logadottir, L. Lindqvist, J. R. Kitchin, T. Bligaard and H. Jónsson, *J. Phys. Chem. B*, 2004, **108**, 17886–17892.

18 S. Piccinin and S. Fabris, *Phys. Chem. Chem. Phys.*, 2011, **13**, 7666–7674.

19 M. Gil-Sepulcre, M. Böhler, M. Schilling, F. Bozoglian, C. Bachmann, D. Scherrer, T. Fox, B. Spingler, C. Gimbert-Suriñach, R. Alberto, R. Bofill, X. Sala, S. Luber, C. J. Richmond and A. Llobet, *ChemSusChem*, 2017, **10**, 4517–4525.